Volumetric Filtering for Shot Gather Interpolation in Swath Seismic Acquisition

Paul Goyes-Peñafiel *Student Member, IEEE,* Edwin Vargas *Student Member, IEEE,* Ymir Mäkinen, Alessandro Foi *Fellow, IEEE,* and Henry Arguello *Senior Member, IEEE*

***Abstract*—Due to environmental and economic constraints inherent to seismic exploration, there are often missing shotpoints and receivers that degrade the resolution of the final seismic image. Hence sophisticated interpolation techniques are required for the recovery of dense and uniform spatial sampling. Recent approaches improve the interpolation by adopting robust models through denoisers. We introduce a 3D shot gather interpolation method that jointly considers a sparse prior and a regularization induced by a multichannel volumetric denoiser. The proposed volumetric regularization uses collaborative filters that perform denoising through transform-domain shrinkage of a group of similar seismic cubes extracted from a land seismic acquisition. This grouping and collaborative filtering paradigm exploit the local correlation present in each cube and the non-local correlation between different cubes. Experiments on the *Stratton 3D survey* show that the proposed method can interpolate 3D shot gathers in an orthogonal seismic recording from a swath geometry, outperforming methods based on 2D denoisers and 5D seismic data reconstruction in terms of root mean square error and in the recovery of seismic reflections.**

***Index Terms*—Shot data reconstruction, BM4D, seismic acquisition, denoiser prior, plug and play denoiser, swath geometry.**

I. Introduction

REGULAR sampling plays an important role in seismic data processing and impacts the imaging quality and interpretation of hydrocarbon exploration. Nevertheless, the sampled seismic data is often incomplete or irregular due to environmental, topographic, or social constraints [1]. Therefore, the missing information must be recovered or interpolated to obtain the regular seismic data. Several reconstruction algorithms are designed for receiver [2], [3] and shot gather recovery [4]–[6] under the assumption that seismic data enjoys an approximate sparse representation with respect to a particular transform or dictionary, such as curvelets, seislets, and atom waves [7]. The reconstruction is further impaired by the random and seismic ambient noise of the acquisition [1], [8]. To improve the interpolation of the seismic data, [9] complements the sparse representation with an implicit data prior implemented as a denoising algorithm under the consensus equilibrium framework [10].

All the above methods for shot gather interpolation have been applied on geometries with a line of shotpoints and a line of receivers, such as the cross-spread, split-spread, and full-spread geometries [5]. In particular, the cross-spread is often used for shot gather interpolation experiments, where the information can be analyzed with high correlation and where sparsity is satisfied [4], [9]. However, Land 3-D acquisition commonly is carried out by swath shooting [11]–[13] in which receiver cables are laid out in parallel lines and shots are positioned in a perpendicular direction [14], and all geophones simultaneously record the elastic energy emitted by a source [15] resulting in a 3D shot gather. Therefore, in this case, previous 2D shot gather interpolation methods cannot account for the 3D structure of the acquired seismic waveform in a missing shot gather. Even though higher dimensional methods exist [3], [16], [17], these have thus far been considered for interpolating missing receivers and not for the interpolation of full 3D shot gathers.

We introduce a 3D shot gather interpolation method that employs a multidimensional regularization model through a volumetric denoiser. Specifically, the denoiser employs the grouping and collaborative filtering paradigm where similar 3D seismic cubes are stacked in a 4D tensor and jointly filtered in a transform domain. This transformation exploits the local correlation present in each cube and the non-local correlation between different cubes leading to an improved separation of signal and noise that cannot be attained by 2D denoisers. We explore the proposed method in a realistic swath seismic acquisition survey where we further leverage the similarity of multiple channels (3D shot gathers) to perform the grouping of the seismic cubes. Numerical results show the improvement in speed and accuracy when compared with interpolation methods that employ 2D denoisers as a regularizer (BM3D–CE) and the 5D interpolation (5D–DRR) using the optimally damped rank–reduction method [17].

II. Acquisition Model using Swath Geometry

A cross–spread configuration consists of a shot line orthogonally intercepted by a receiver line Figure 1(a), resulting in a 3D seismic survey as shown in Figure 1(b) composed by M stacked 2D shot gathers. However, in practice, the seismic acquisition is performing juxtaposition of cross–spreads [15]. Hence, recording the seismic signal for a shot employs several lines of receivers simultaneously in a multi–orthogonal seismic acquisition called swath geometry [12], as illustrated in

This work was supported by project 110287780575 through the agreement 785-2019 between ANH, MINCIENCIAS, Fondo Francisco José de Caldas, and by the Academy of Finland (project no. 336357, PROFI 6 - TAU Imaging Research Platform).

P. Goyes-Peñafiel and H. Arguello are with the Department of Systems Engineering, Universidad Industrial de Santander, Bucaramanga 680002, Colombia (e-mail: ypgoype@correo.uis.edu.co; henarfu@uis.edu.co)

E. Vargas is with the Department of Electronics Engineering, Universidad Industrial de Santander, Bucaramanga, Colombia. (e-mail: edwin.vargas4@correo.uis.edu.co)

Y. Mäkinen and A. Foi are with the Faculty of Information Technology and Communication Sciences, Tampere University, 33720 Tampere, Finland (e-mail: ymir.makinen@tuni.fi; alessandro.foi@tuni.fi).

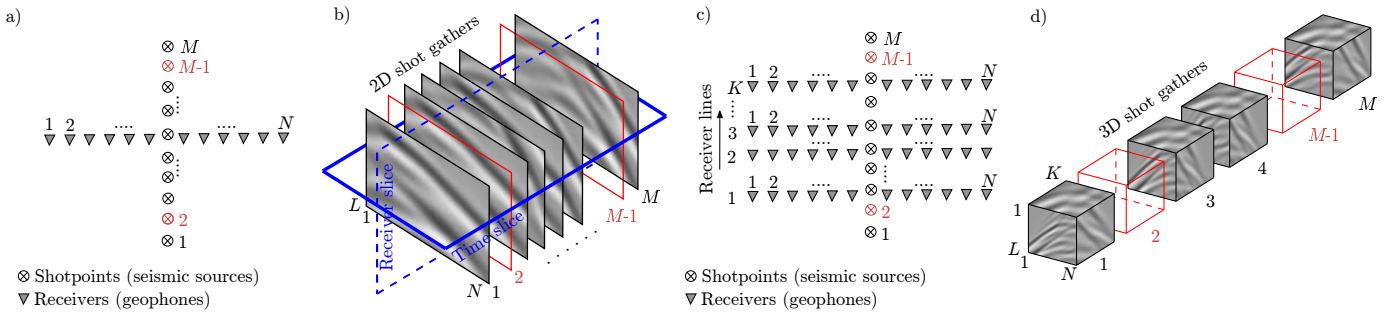

Fig. 1. (a) Cross–spread [4], [9] and (c) swath geometry [12]. (b) and (d) are the 3D and 4D tensor representation for the subsampled acquisitions from (a) and (c) respectively by removing the shotpoints at 2 and $M-1$.

Figure 1(c). Therefore, in this case, the seismic data can be represented as 4–D structures comprising L samples in time of the reflected energy emitted by M shot gathers, captured by a sequence of K receiver lines with N receivers per line. Here, a single shot gather is recorded by an $L \times N \times K$ array as shown Figure 1(d). Additionally, swath geometry preserves the advantages of a cross–spread and provides seismic signals with less random noise [4].

The acquisition process illustrated in Figure 1(c) can be modeled as a system of linear equations given by

$$\mathbf{y} = \mathbf{\Phi}\mathbf{x} + \boldsymbol{\omega}, \tag{1}$$

where $\mathbf{\Phi} \in \mathbb{R}^{LNK(M-k)\times LNKM}$ being the acquisition operator, $\mathbf{x} \in \mathbb{R}^{LNKM}$ is the vector representation of the M 3D shot gathers in Figure 1(d) and $\boldsymbol{\omega}$ accounts for the acquisition noise. $\mathbf{\Phi} \in \mathbb{R}^{LNK(M-k)\times LNKM}$ is defined as $\mathbf{\Phi} = \mathbf{S} \otimes \mathbf{I}_{LNK}$, where $\otimes$ represents the Kronecker product [18], $\mathbf{I}_{LNK}$ is a $LNK \times LNK$ identity matrix, $\mathbf{S} \in \mathbb{R}^{M-k\times M}$ model the shot subsampling effect and is obtained by removing from the identity matrix $\mathbf{I}_M$, k rows corresponding to the k missing shot gathers. The acquired shot gathers $\mathbf{y}$ are then used to estimate the whole data set $\mathbf{x}$.

III. Volumetric Shot Gather Interpolation

For the estimation, the traditional CS formulation exploits the sparse representation of $\mathbf{x}$ on a given transform basis $\mathbf{D} \in \mathbb{R}^{LNKM\times LNKM}$ such as wavelets or curvelets [19], with the estimate $\hat{\mathbf{x}}$ of $\mathbf{x}$ defined as the solution of

$$\hat{\mathbf{x}} = \arg\min_{\mathbf{x}} \ \tfrac{1}{2}||\mathbf{y} - \mathbf{\Phi}\mathbf{x}||_2^2 + \lambda||\mathbf{D}\mathbf{x}||_1 \ , \tag{2}$$

where the parameter $\lambda > 0$ balances the quadratic fidelity versus the ℓ_1 sparsity penalty.

Although the sparsity promoted with the ℓ_1-norm has been widely used in seismic applications [4], [5], a recent work [9] explored combining sparsity and Plug and Play (PnP) priors to improve the reconstruction. PnP priors have been studied as a mechanism for incorporating image denoisers as implicit regularizations for inverse problems [20], [21]. The interpolated seismic data in [9] is the solution to the following optimization problem

$$\hat{\mathbf{x}} = \arg\min_{\mathbf{x}} \ \tfrac{1}{2}||\mathbf{y} - \mathbf{\Phi}\mathbf{x}||_2^2 + \lambda||\mathbf{D}\mathbf{x}||_1 + \beta h(\mathbf{x}) \ , \tag{3}$$

where λ and β are regularization parameters and h is the implicit PnP regularization function defined by the Block-Matching and 3D filtering (BM3D) denoiser. However, since BM3D is a 2D denoiser, the regularization defined by BM3D is applied through 2D dimensional structures of the seismic data cube and therefore, as a PnP prior, it cannot take full advantage of the higher dimensional structure of the seismic waveform (i.e. the multiples cubes in Figure 1(d) correspond to a 4D tensor acquired in a swath acquisition geometry).

Here, we propose to interpolate missing shot gathers of the target (pre–plot) swath geometry in land seismic acquisitions using (3) and the *volumetric multichannel BM4D denoiser* [22], [23] as PnP prior instead of BM3D. Similar to [9], we address (3) using the *Consensus Equilibrium (CE) approach* [10], [24] that solves a generalized inverse problem that includes multiple data fitting and regularization terms. Within CE, we use BM4D iteratively on an auxiliary variable $\mathbf{v}_k$ to pull the current estimate $\hat{\mathbf{x}}_k$ toward a solution $\hat{\mathbf{x}}$ with improved regularity of similar seismic structures along the M 3D shot gathers. In the following, we present in detail the *multichannel denoising algorithm in the context of multiple receiver lines acquisition.*

A. Collaborative filtering of volumetric multichannel data

1) Noise model: The input $\mathbf{v}_k$ of the denoiser is multichannel volumetric (i.e. 4D) data structured as in Figure 1(d). Specifically, we model $\mathbf{v}_k$ as a noisy realization of $\mathbf{x}$

$$\mathbf{v}_k = \mathbf{x} + \mathbf{n}_k, \qquad \mathbf{n}_k\left(\cdot\right) \sim \mathcal{N}\left(0, \sigma_k^2\right), \tag{4}$$

where $\mathbf{n}_k$ is zero–mean i.i.d. Gaussian noise with variance σ_k^2. The goal of the filtering is then to estimate $\mathbf{x}$ from $\mathbf{v}_k$.

2) Multichannel BM4D filtering: The land seismic acquisition is performed by a swath shooting sequence over a multi–orthogonal geometry, which consists of all receivers that are actively recording for a given shot point [15]. Due to the parallel nature of receiver lines within a swath geometry, shot gathers capture waveform shapes and seismic signal structures that repeat in the majority of the records such as reflection hyperbolas, ground roll waves (surface waves), and refraction (linear events). Therefore, there are similar structures between the different seismic shots, which are exploited to use algorithms that can find those areas of high similarities, such as BM4D. We adopt directly the BM4D implementation

of [23] applied as a multichannel denoiser across principal components computed across the shot gathers, extending the 2D multichannel approach of [25] to 4D data.

We begin the denoising by *computing the principal components* (PC) across the M 3D shot gathers that form $\mathbf{v}_k$, resulting in M 3D PCs, which we regard as the channels for BM4D denoising. BM4D processes the data in groups of small $4\times4\times4$ cubes extracted from the individual channels according to the following scheme.

The first PC has the highest signal–to–noise ratio among the PCs and $\mathbf{v}_k$. Hence, we select this channel to evaluate *cube-matching*, identifying volumetric positions of similar cubes. Then, individually for each channel, we build groups of similar cubes collected from the positions indicated by the cube-matching, as illustrated in Figure 2. Each group of cubes is organized into a 4D structure by stacking the cubes along a nonlocal 4th dimension. As the common broader structures persist across the channels, also the groups built for channels other than the first one enjoy high internal self-similarity.

We *transform* each group of cubes, obtaining 4D spectra in which the underlying regular structures are extremely sparsely represented because of self-similarity between the grouped cubes. Due to this sparsity, by *shrinkage* of the 4D spectra, we attenuate the noise while preserving most of the underlying signal and enhancing both local and non-local regularity across the multiple channels.

After shrinkage, *the 4D group transform is inverted*, and each resulting cube estimate is *aggregated* into the corresponding channel at its original position. In this way, we form a denoised estimate of the M channels.

Finally, the *inverse PCA* with respect to the M channels returns a denoised estimate of the M 3D shot gathers.

Note that the above denoising procedure operates across five dimensions, decorrelating the 4D data (as shown in Figure 1d) through a data–driven 5D highly redundant transform resulting from PCA and groupwise 4D transforms. The extra dimension corresponds to the nonlocal dimension along which we encode the similarity of grouped blocks.

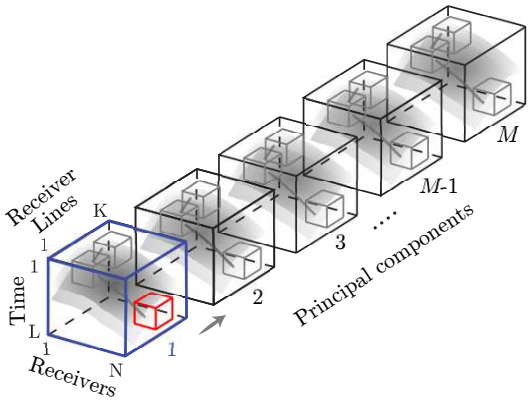

Fig. 2. Illustration of multichannel BM4D cube-matching for different PCs of $\mathbf{v}_k$, showing the matching of three cubes. The cube-matching is performed only on the first PC; the resulting cube positions are then repeated across every component $1,\ldots,M$ to form the corresponding groups of cubes.

TABLE I
RMSE SUMMARY FOR THE MISSING 3D SHOT GATHERS 4, 6, AND 9 INTERPOLATED BY THE PROPOSED METHOD, BM3D–CE [9], AND 5D–DRR [17].

Shot index	Proposed	BM3D–CE	5D–DRR
4	**0.005** ± 0.001	0.035 ± 0.005	0.172 ± 0.007
6	**0.004** ± 0.002	0.026 ± 0.007	0.194 ± 0.013
9	**0.005** ± 0.001	0.043 ± 0.008	0.203 ± 0.019
{4, 6, 9}	**0.0046** ± 0.0015	0.0346 ± 0.006	0.1896 ± 0.0130
Run time	1330 s	6600 s	2600 s

IV. Simulations and Results

The experiments to evaluate the proposed volumetric denoising regularization for shot gather interpolation were performed using the *Stratton 3D survey* [26], specifically using a Swath corresponding to source line 556. The data acquisition consists of a multi–orthogonal land seismic survey in the south of Texas. The swath acquisition parameters are: $M=10$ 3D shot gathers, $K=6$ receiver lines with $N=112$ receivers and $L=500$ time samples. We simulate $k=3$ missing shotpoints at positions $4, 6, 9$ and initialize the missing shot gathers as zero. We used the 3D wavelet transform symlet–8 as dictionary $\mathbf{D}$ for the sparse representation used in (3). The 3D wavelet transform is applied in the receiver line direction, where for each receiver line, cubes of dimension $L \times N \times M$ are configured. Our results were compared with those obtained by the competitive BM3D–CE [9] and 5D–DRR [17] methods. The root–mean–square error (RMSE) is used as the objective metric to assess the accuracy of the interpolated 3D shot gathers. The method's parameters are tuned in order to minimize the RMSE; in particular, for the proposed method we tuned the noise variance assumed by BM4D (σ_k, fixed for all k for simplicity) and the regularization parameters in (3) (λ, β) via the grid search tool from [27], obtaining values $\sigma_k = 10^{-5}$, $\beta = 8\cdot10^{-3}$, and $\lambda = 10^{-4}$. For 5D-DRR the missing data was initialized with a spline interpolation. Furthermore, following [17], we used the *denoising and interpolation* mode of 5D–DRR with rank= 24 to account for the nonlinear seismic events.

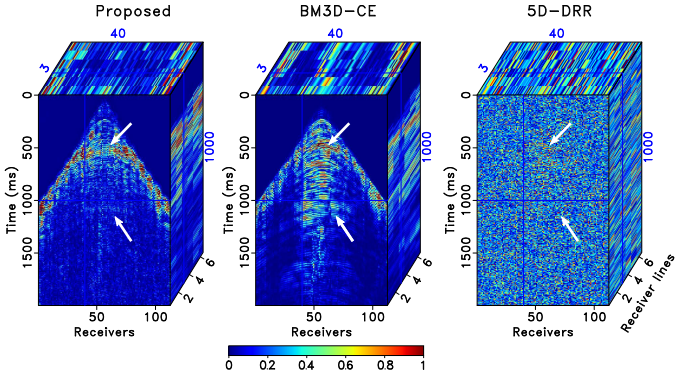

Fig. 3. 3D Absolute differences between the original shot gather 4 and those interpolated by the proposed, BM3D-CE and 5D-DRR methods. Note that the slices are at 1000 ms, receiver 40, and receiver line 3, respectively.

Table I summarizes the interpolation results of the missing 3D shots gathers 4, 6, and 9 in terms of average RMSE over

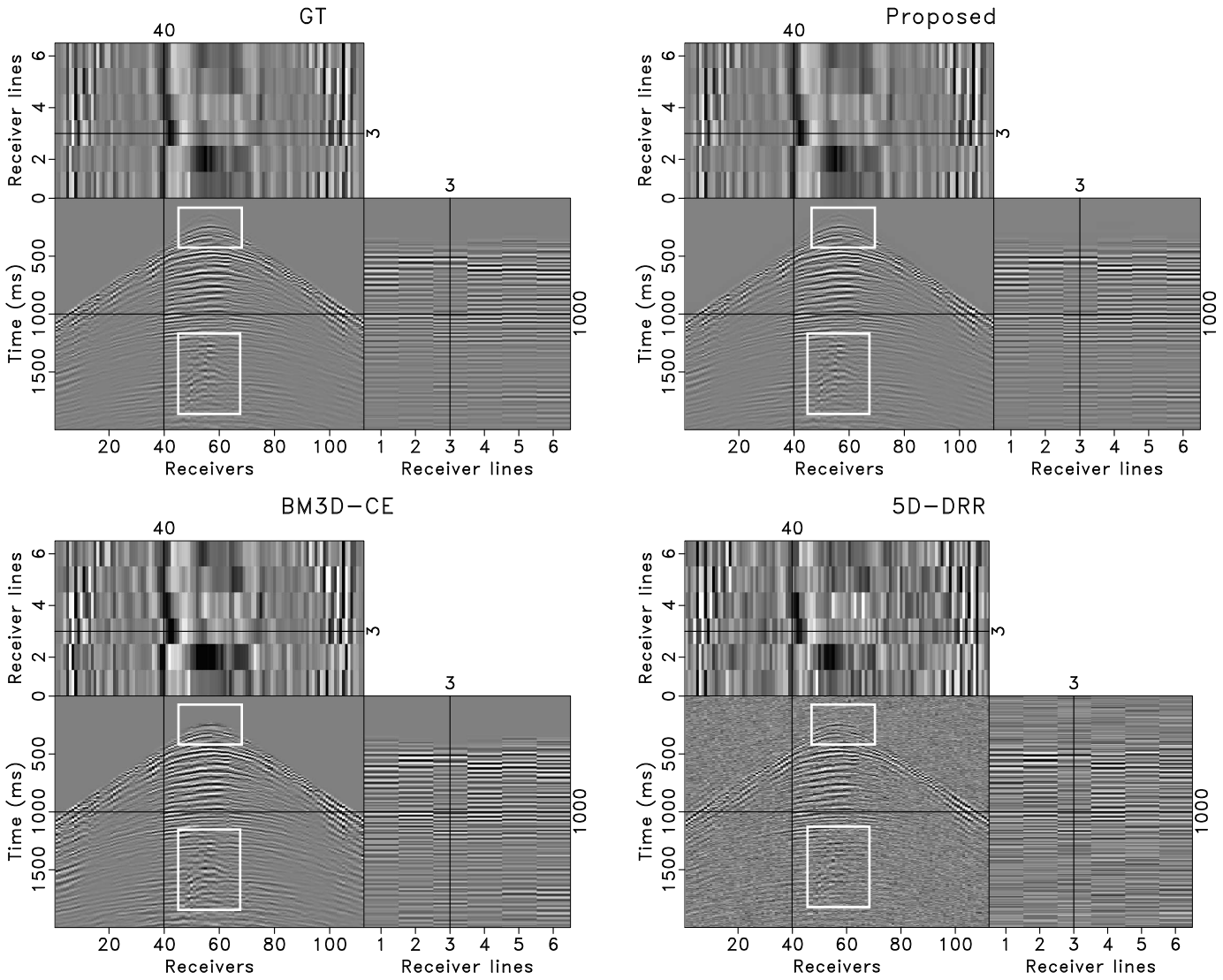

Fig. 4. Comparison of the interpolated 3D shot gather 4 using the slices at time 1000 ms, receiver 40, and receiver line 3. The white box highlights the ground roll accurately reconstructed by the proposed method. The upper box shows the first arrivals omitted by the BM3D–CE method.

the 6 receiver lines within each single interpolated 3D shot gather, as well as over all 18 receiver slices in the three 3D shot gathers, along with the corresponding standard deviation. The proposed method shows a better performance in all interpolated 3D shot gathers. We also report the corresponding run times on a AMD Ryzen 7 5800X3D CPU on a single core and 128 GB RAM. The proposed method is highly efficient, also thanks to the PCA which allows to alleviate the computational burden of the cube–matching, evaluated only once on the first PC, instead of performing it separately on each channel. The low errors are visualized in Figure 3, where the proposed method presents localized high errors near the linear events of the first arrivals primarily due to slight changes in the reconstructed amplitude, in contrast to the BM3D–CE method that concentrates its highest errors in the central part of the shot gather due to poor reconstruction of the ground roll in both amplitude and shape pointed with the arrows.

Figure 4 provides a visual comparison of the 3D shot gather 4 interpolated by the different methods. This visual inspection confirms the results in the table, and it can be observed that BM3D–CE fails to interpolate internal seismic structures such as linear events related to the first arrivals and that 5D–DRR recovers the structures, but is highly contaminated with noise. Overall, our method provides a better reconstruction of seismic amplitudes and a smoother lateral continuity for seismic events including coherent noise. We evaluated the reconstruction quality of the different methods by extracting receiver 40 from shot gather 4 of the receiver line 3, as illustrated in Figure 5. The analysis window ranges from 1240 ms to 1400 ms, and it is evident that the proposed method provides accurate alignment with all measurement points, especially in regions with high curvature. In contrast, the BM3D–CE method exhibited incorrect amplitude estimation of the waveform in these areas.

We finally note that, as reported by [9], the sparsity prior helps in the recovery of the low–frequency components of the shot gathers and the estimation with only the denoising regularization (i.e. $\lambda = 0$) also leads to inferior results due

to the complexity of shapes related with nonlinear seismic events. As already commented, the PCA is beneficial for improving the matching and thus the sparsity, as well as for decreasing complexity; in particular, if each shot gather had been processed independently by (single–channel) BM4D, the RMSE and run–time would approximately increase by 20% and by 50%, respectively.

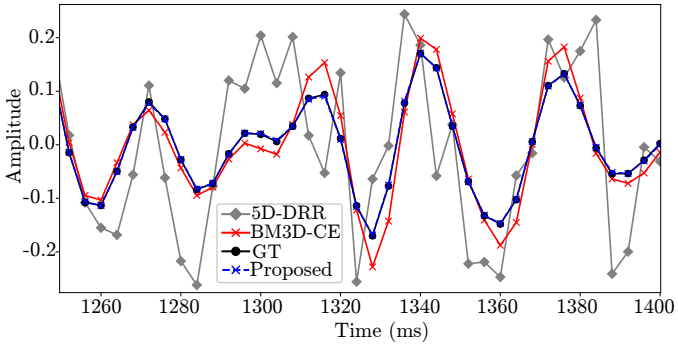

Fig. 5. Detailed waveform between 1240 and 1400 ms located on receiver 40, shot gather 4, receiver line 3. The proposed method achieves the best fitting, especially in areas with higher curvature.

V. Conclusion

This paper proposes to employ a volumetric denoising regularizer and sparsity prior to 3D shot gather interpolation sampled simultaneously in several receiver lines. Because reflections always occur over a finite set of reflectors at depth and some seismic characteristics are repeated in the swath seismic acquisition, the proposed method exploits multichannel collaborative filtering of similar seismic volumes to improve the interpolation of typical 3D events. Experiment results on *Stratton 3D survey* dataset showed the advantages of the proposed approach compared with leading competitive methods in a scenario of 3D missing shots. Particularly, our approach provides lower RMSE and superior quality in the recovery of both linear and nonlinear seismic events, and with less computational time.

Acknowledgment

The authors thank the Centre for High–Performance Computing and the High Dimensional Signal Processing research group at Universidad Industrial de Santander, and NVIDIA Academic Hardware Grant Program for providing computational resources to run the parameter tuning experiments.

References

[1] A. Titova, M. B. Wakin, and A. Tura, "Two-stage sampling – A novel approach for compressive sensing seismic acquisition," *SEG Technical Program Expanded Abstracts*, pp. 110–114, 2021.

[2] T. Jiang, B. Gong, F. Qiao, Y. Jiang, A. Chen, D. Hren, and Z. Meng, "Compressive seismic reconstruction with extended POCS for arbitrary irregular acquisition," in *SEG Technical Program Expanded Abstracts 2017*. SEG, aug 2017, pp. 4272–4277.

[3] D. Trad, "Five-dimensional interpolation: Recovering from acquisition constraints," *Geophysics*, vol. 74, no. 6, pp. V123–V132, 2009.

[4] O. Villarreal, K. León-López, D. Espinosa, W. Agudelo, and H. Arguello, "Seismic source reconstruction in an orthogonal geometry based on local and non-local information in the time slice domain," *J. Applied Geophysics*, vol. 170, p. 103846, 2019.

[5] L. Galvis, J. M. Ramírez, E. Vargas, O. Villarreal, W. Agudelo, and H. Arguello, "Reconstruction of 2D Seismic Wavefields from Nonuniformly Sampled Sources," *Electronic Imaging*, vol. 2020, pp. 307–307, 2020.

[6] O. P. Villarreal, K. Leon, D. Espinosa, W. Agudelo, and H. Arguello, "Compressive sensing seismic acquisition by using regular sampling in an orthogonal grid," in *2017 IEEE 7th International Workshop on Computational Advances in Multi-Sensor Adaptive Processing (CAMSAP)*. IEEE, 2017, pp. 1–5.

[7] S. R. Borra, G. J. Reddy, and E. S. Reddy, "Seismic Data Compression using Wave Atom Transform," *Global J. Computer Science and Technology: F Graphics and Vision*, vol. 15, no. 1, pp. 35–41, 2015.

[8] L. Zhu, E. Liu, and J. H. McClellan, "Seismic data denoising through multiscale and sparsity-promoting dictionary learning," *Geophysics*, vol. 80, no. 6, pp. WD45–WD57, 2015.

[9] P. Goyes-Peñafiel, E. Vargas, C. V. Correa, W. Agudelo, B. Wohlberg, and H. Arguello, "A Consensus Equilibrium Approach for 3-D Land Seismic Shots Recovery," *IEEE Geosci. Remote Sens. Lett*, pp. 1–5, 2022.

[10] G. T. Buzzard, S. H. Chan, S. Sreehari, and C. A. Bouman, "Plug-and-Play Unplugged: Optimization-Free Reconstruction Using Consensus Equilibrium," *SIAM J. Imaging Sciences*, vol. 11, pp. 2001–2020, 2018.

[11] Ö. Yilmaz, *Seismic Data Analysis*. Society of Exploration Geophysicists, jan 2001. [Online]. Available: https://library.seg.org/doi/book/10.1190/1.9781560801580

[12] Y. Wang and Z. Yang, "Application effects of swath 3D geometry in the foothill regions of western China," *J. Seismic Exploration*, vol. 28, pp. 347–361, 2019.

[13] A. Cordsen, M. Galbraith, and J. Peirce, *Planning Land 3-D Seismic Surveys*. Society of Exploration Geophysicists, 2000.

[14] C. L. Liner, "Chapter 10: Land Shooting Geometry," in *Elements of 3D Seismology*. Society of Exploration Geophysicists, jan 2016, pp. 111–122. [Online]. Available: https://library.seg.org/doi/10.1190/1.9781560803386.ch10

[15] A. Chaouch and J. L. Mari, "3-D Land Seismic Surveys: Definition of Geophysical Parameter," *Oil & Gas Science and Technology - Revue de l'IFP*, vol. 61, pp. 611–630, 2006.

[16] L. Zhang, A. Li, J. Yang, S. Li, Y. Yao, F. Xiao, and Y. Huang, "Five-dimensional interpolation in the OVT domain for wide-azimuth seismic data," *J. Geophysics and Engineering*, vol. 18, pp. 529–538, 2021.

[17] Y. Chen, M. Bai, Z. Guan, Q. Zhang, M. Zhang, and H. Wang, "Five-dimensional seismic data reconstruction using the optimally damped rank-reduction method," *Geophysical Journal International*, vol. 222, pp. 1824–1845, 2020.

[18] H. Zhang and F. Ding, "On the Kronecker products and their applications," *Journal of Applied Mathematics*, vol. 2013, pp. 1–8, 2013.

[19] F. J. Herrmann, M. P. Friedlander, and Ö. Yilmaz, "Fighting the curse of dimensionality: Compressive sensing in exploration seismology," *IEEE Signal Processing Magazine*, vol. 29, pp. 88–100, 2012.

[20] Y. Romano, M. Elad, and P. Milanfar, "The little engine that could: Regularization by denoising (RED)," *SIAM J. Imaging Sciences*, vol. 10, no. 4, pp. 1804–1844, 2017.

[21] S. V. Venkatakrishnan, C. A. Bouman, and B. Wohlberg, "Plug-and-Play priors for model based reconstruction," in *2013 IEEE Global Conference on Signal and Information Processing*. IEEE, 2013, pp. 945–948.

[22] M. Maggioni, V. Katkovnik, K. Egiazarian, and A. Foi, "Nonlocal Transform-Domain Filter for Volumetric Data Denoising and Reconstruction," *IEEE Trans. Image Process.*, vol. 22, pp. 119–133, 2013.

[23] Y. Mäkinen, S. Marchesini, and A. Foi, "Ring artifact and Poisson noise attenuation via volumetric multiscale nonlocal collaborative filtering of spatially correlated noise," *J. Synchrotron Radiation*, vol. 29, no. 3, pp. 829–842, 2022.

[24] S. Muramatsu, S. Chai, S. Ono, T. Ota, F. Nin, and H. Hibino, "Oct Volumetric Data Restoration via Primal-Dual Plug-and-Play Method," *ICASSP, IEEE Int. Conf. Acoustics, Speech and Signal Processing - Proceedings*, vol. 2018-April, pp. 801–805, 2018.

[25] T. Gelvez-Barrera, H. Arguello, and A. Foi, "Joint Nonlocal, Spectral, and Similarity Low-Rank Priors for Hyperspectral–Multispectral Image Fusion," *IEEE Trans. Geosci. and Remote Sens.*, vol. 60, pp. 1–12, 2022.

[26] B. Hardage and S. Tinker, "Stratton 3D survey," https://dataunderground.org/no/dataset/stratton, 2021, online; accessed 29 January 2021.

[27] B. Wohlberg, "SPORCO: A Python package for standard and convolutional sparse representations," in *Proceedings of the 16th Python in Science Conference (SCIPY 2017)*, K. Huff, D. Lippa, D. Niederhut, and M. Pacer, Eds., 2017, pp. 1–8.